Monocrystalline silicon carbide nanoelectromechanical systems

Y. T. Yang, K. L. Ekinci, X. M. H. Huang, L. M. Schiavone, and M. L. Roukes[a)]
Condensed Matter Physics 114-36, California Institute of Technology, Pasadena, California 91125

C. A. Zorman and M. Mehregany
Department of Electrical Engineering and Computer Science, Case Western Reserve University, Cleveland, Ohio 44106

(Received 21 August 2000; accepted for publication 15 November 2000)

SiC is an extremely promising material for nanoelectromechanical systems given its large Young's modulus and robust surface properties. We have patterned nanometer scale electromechanical resonators from single-crystal 3C-SiC layers grown epitaxially upon Si substrates. A surface nanomachining process is described that involves electron beam lithography followed by dry anisotropic and selective electron cyclotron resonance plasma etching steps. Measurements on a representative family of the resulting devices demonstrate that, for a given geometry, nanometer-scale SiC resonators are capable of yielding substantially higher frequencies than GaAs and Si resonators. © *2001 American Institute of Physics.* [DOI: 10.1063/1.1338959]

Silicon carbide is an important semiconductor for high temperature electronics due to its large band gap, high breakdown field, and high thermal conductivity. Its excellent mechanical and chemical properties have also made this material a natural candidate for microsensor and microactuator applications in microelectromechanical systems (MEMS).[1]

Recently, there has been a great deal of interest in the fabrication and measurement of semiconductor devices with fundamental mechanical resonance frequencies reaching into the microwave bands. Among technological applications envisioned for these nanoelectromechanical systems (NEMS) are ultrafast, high-resolution actuators and sensors, and high frequency signal processing components and systems.[2] From the point of view of fundamental science, NEMS also offer intriguing potential for accessing regimes of quantum phenomena and for sensing at the quantum limit.

SiC is an excellent material for high frequency NEMS for two important reasons. First, the ratio of its Young's modulus, E, to mass density, ρ, is significantly higher than for other semiconducting materials commonly used for electromechanical devices, e.g., Si and GaAs. Flexural mechanical resonance frequencies for beams directly depend upon the ratio $\sqrt{(E/\rho)}$. The goal of attaining extremely high fundamental resonance frequencies in NEMS, while simultaneously preserving small force constants necessary for high sensitivity, requires pushing against the ultimate resolution limits of lithography and nanofabrication processes. SiC, given its larger $\sqrt{(E/\rho)}$, yields devices that operate at significantly higher frequencies for a given geometry, than otherwise possible using conventional materials. Second, SiC possesses excellent chemical stability.[3] This makes surface treatments an option for higher quality factors (Q factor) of resonance. It has been argued that for NEMS the Q factor is governed by surface defects and depends on the device surface-to-volume ratio.[2]

Micron-scale SiC MEMS structures have been fabricated using both bulk and surface micromachining techniques. Bulk micromachined 3C-SiC diaphragms, cantilever beams, and torsional structures have been fabricated directly on Si substrates using a combination of 3C-SiC growth processes and conventional Si bulk micromachining techniques in aqueous KOH[4] and TMAH solutions.[5] Surface micromachined SiC devices have primarily been fabricated from polycrystalline 3C-SiC (poly-SiC) thin films deposited directly onto silicon dioxide sacrificial layers, patterned using reactive ion etching, and released by timed etching in aqueous hydrofluoric acid solutions.[6] Single crystal 3C-SiC surface micromachined structures have been fabricated in a similar way from 3C-SiC-on-SiO_2 substrates created using wafer bonding techniques.[7] We have developed an alternative approach for nanometer-scale single crystal, 3C-SiC layers that is not based upon wet chemical etching and/or wafer bonding. Especially noteworthy is that our final suspension step in the surface nanomachining process is performed by using a dry etch process. This avoids potential damage due to surface tension encountered in wet etch processes, and circumvents the need for critical point drying when defining large, mechanically compliant devices. We first describe the method we developed for fabrication of suspended SiC structures, then demonstrate the high frequency performance attained from doubly clamped beams read out using magnetomotive detection.

The starting material for device fabrication is a 259-nm-thick single crystalline 3C-SiC film heteroepitaxially grown on a 100 mm diameter (100) Si wafer. 3C-SiC epitaxy is performed in a rf induction-heated reactor using a two-step, carbonization-based atmospheric pressure chemical vapor deposition (APCVD) process detailed elsewhere.[8] Silane and propane are used as process gases and hydrogen is used as the carrier gas. Epitaxial growth is performed at a susceptor temperature of about 1330 °C. 3C-SiC films grown using this process have a uniform (100) orientation across each wafer, as indicated by x-ray diffraction. Transmission electron microscopy and selective area diffraction analysis indicates that the films are single crystalline. The microstructure is typical of epitaxial 3C-SiC films grown on Si substrates, with the

[a)]Electronic mail: roukes@cal.tech.edu

Downloaded 05 Jan 2001 to 131.215.106.152. Redistribution subject to AIP copyright, see http://ojps.aip.org/aplo/aplcpyrts.html.

largest density of defects found near the SiC/Si interface, which decreases with increasing film thickness. A unique property of these films is that the 3C-SiC/Si interface is absent of voids, a characteristic not commonly reported for 3C-SiC films grown by APCVD.

Fabrication begins by defining large area contact pads by optical lithography. A 60-nm-thick layer of Cr is then evaporated and, subsequently, standard lift-off is carried out with acetone. Samples are then coated with a bilayer poly(methylmethacrylate (PMMA) resist prior to patterning by electron beam lithography. After resist exposure and development, 30–60 nm of Cr is evaporated on the samples, followed by lift-off in acetone. The pattern in the Cr metal mask is then transferred to the 3C-SiC beneath it by anisotropic electron cyclotron resonance (ECR) plasma etching. We use a plasma of NF_3, O_2, and Ar at a pressure of 3 mTorr with respective flow rates of 10, 5, 10 sccm, and a microwave power of 300 W. The acceleration dc bias is 250 V. The etch rate under these conditions is ~65 nm/min.

The vertically etched structures are then released by controlled local etching of the Si substrate using a selective isotropic ECR etch for Si. We use a plasma of NF_3 and Ar at a pressure of 3 mTorr, both flowing at 25 sccm, with a microwave power 300 W, and a dc bias of 100 V. We find that NF_3 and Ar alone do not etch SiC at a noticeable rate under these conditions. The horizontal and vertical etch rates of Si are ~300 nm/min. These consistent etch rates enable us to achieve a significant level of control of the undercut in the clamp area of the structures. The distance between the suspended structure and the substrate can be controlled to within 100 nm.

After the structures are suspended, the Cr etch mask is removed either by ECR etching in an Ar plasma or by a wet Cr photomask etchant (perchloric acid and ceric ammonium nitrate). The chemical stability and the mechanical robustness of the structures allow us to perform subsequent lithographic fabrication steps for the requisite metallization (for magnetomotive transduction) step on the *released* structures. Suspended samples are again coated with bilayer PMMA and after an alignment step, patterned by electron beam lithography to define the desired electrodes. The electrode structures are completed by thermal evaporation of 5-nm-thick Cr and 40-nm-thick Au films, followed by standard lift-off. Finally, another photolithography step, followed by evaporation of 5 nm Cr and 200 nm Au and conventional lift-off, is performed to define large contact pads for wire bonding. Two examples of completed structures, each containing a family of doubly clamped SiC beams of various aspect ratios, are shown in Fig. 1.

We have measured the fundamental resonance frequencies of both the in-plane and out-of-plane vibrational modes for a family of doubly clamped SiC beams, with rectangular cross section and different aspect ratios (length/width). Samples were glued into a chip carrier and electrical connections were provided by Al wirebonds. Electromechanical characteristics were measured using the magnetomotive detection technique[9] from 4.2 to 295 K, in a superconducting solenoid within a variable temperature cryostat. The measured fundamental frequencies in this study ranged from 6.8 to 134 MHz. The quality factors, extracted from the fundamental mode resonances for each resonator, range from $10^3 < Q < 10^4$. Figure 2 shows the response of one representative beam with dimensions 8 μm (length) × 600 nm (width) × 259 nm (thickness). This particular device yields an in-plane resonant frequency of 71.91 MHz and a $Q \sim 4000$ at 20 K. Quality factors at room temperature were typically a factor of 4–5 smaller than values obtained at low temperature.

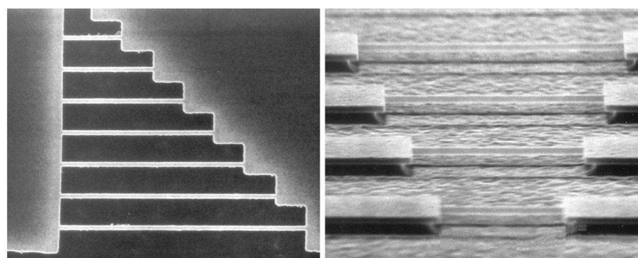

FIG. 1. Doubly clamped SiC beams patterned from a 259-nm-thick epilayer. (left) Top view of a family of 150 nm wide beams, having lengths from 2 to 8 μm. (right) Side view of a family of 600 nm wide beams, with lengths ranging from 8 to 17 μm.

We now demonstrate the benefits of SiC for NEMS, by directly comparing frequencies attainable for structures of similar geometry made with SiC, Si, and GaAs. The fundamental resonance frequency, f, of a doubly clamped beam of length, L, and thickness, t, varies linearly with the geometric factor t/L^2 according to the simple relation

$$f = 1.03 \sqrt{\frac{E}{\rho}} \frac{t}{L^2}, \tag{1}$$

where E is the Young's modulus and ρ is the mass density. In our devices the resonant response is not so simple, as the added mass and stiffness of the metallic electrode modify the resonant frequency of the device. This effect becomes particularly significant as the beam size shrinks. To separate the primary dependence upon the structural material from secondary effects due to electrode loading and stiffness, we employ a simple model for the composite vibrating beam.[10] In

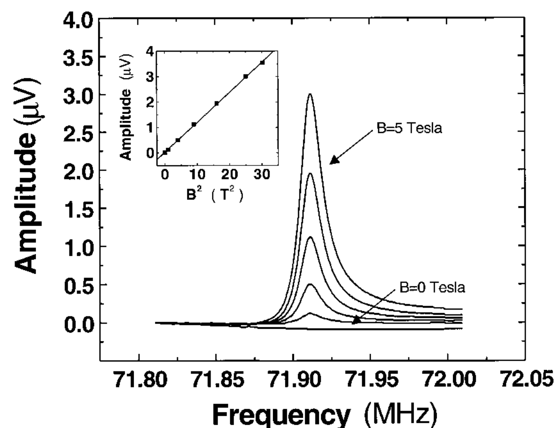

FIG. 2. Representative data; a SiC doubly clamped beam resonating at 71.91 MHz, with quality factor $Q \sim 4000$. The family of resonance curves are taken at various magnetic fields; the inset shows the characteristic B^2 dependence expected from magnetomotive detection. For clarity of presentation here the data is normalized to response at zero magnetic field, with the electrode's dc magnetoresistance shift subtracted from the data; these provide an approximate means for separating the electromechanical response from the that of the passive measurement circuitry.

Downloaded 05 Jan 2001 to 131.215.106.152. Redistribution subject to AIP copyright, see http://ojps.aip.org/aplo/aplcpyrts.html.

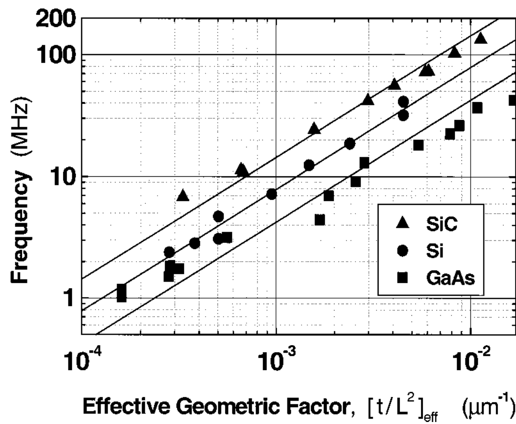

FIG. 3. Frequency vs effective geometry for three families of doubly clamped beams made from single-crystal SiC, Si, and GaAs. All devices are patterned to have the long axis of the device along ⟨100⟩. Ordinate are normalized to remove the effect of additional stiffness and mass loading from electrode metallization. The solid lines are least squares fits assuming unity slope, and yield values of the parameter $v=\sqrt{E/\rho}$ that closely match expected values.

general, for a beam comprised of two layers of different materials the resonance equation is modified to become

$$f=\frac{\eta}{L^2}\left(\frac{E_1I_1+E_2I_2}{\rho_1A_1+\rho_2A_2}\right)^{1/2}. \quad (2)$$

Here the indices 1 and 2 refer to the geometric and material properties of the structural and electrode layers, respectively. The constant η depends upon mode number and boundary conditions; for the fundamental mode of a doubly clamped beam $\eta=3.57$. Assuming the correction due to the electrode layer (layer 2) is small, we can define a correction factor K, to allow direct comparison with the expression for homogeneous beam

$$f=\frac{\eta}{L^2}\left(\frac{E_1I_{10}}{\rho_1A_{10}}\right)^{1/2}, \text{ where } K=\frac{E_1I_1+E_2I_2}{E_1I_{10}}\frac{1}{1+\dfrac{\rho_2A_2}{\rho_1A_2}}. \quad (3)$$

In this expression, I_{10} is the moment calculated in the absence of the second layer. The correction factor K can then be used to obtain a value for the *effective geometric factor*, $[t/L^2]_{\text{eff}}$, for the measured frequency.[11] Further nonlinear correction terms, of order higher than $[t/L^2]_{\text{eff}}$, are expected to appear if the beams are under significant tensile or compressive stress. The linear trend of our data, however, indicates that internal stress corrections to the frequency are small.

In Fig. 3, we display the measured resonance frequencies as a function of $[t/L^2]_{\text{eff}}$ for beams made of three different materials: GaAs, Si and SiC.[12] The lines in this logarithmic plot represent least squares fits to the data assuming unity slope. From these we can deduce the effective values of the parameter, $v=\sqrt{(E/\rho)}$, which is similar (but not identical) to the velocity of sound for the three materials.[13] The numerical values obtained by this process are: $v(\text{SiC})=1.5\times10^4$ m/s, $v(\text{Si})=8.4\times10^3$ m/s, and $v(\text{GaAs})=4.4\times10^3$ m/s. These are quite close to values calculated from data found in the literature: $v(\text{SiC})=1.2\times10^4$ m/s,[14] $v(\text{Si})=7.5\times10^3$ m/s,[15] and $v(\text{GaAs})=4.0\times10^3$ m/s,[16] respectively. The small discrepancies are consistent with our uncertainties in determining both the exact device geometries and the precise perturbation of the mechanical response arising from the metallic electrodes. Nonetheless, SiC very clearly exhibits the highest $\sqrt{(E/\rho)}$ ratio.

In conclusion, we report a simple method for fabricating nanomechanical devices from single-crystal 3C-SiC materials. We demonstrate patterning mechanical resonators using a single metal mask, and just two steps of ECR etching. Our results illustrate that SiC is an ideal semiconductor with great promise for device applications requiring high frequency mechanical response.

The authors gratefully acknowledge support for this work from DARPA MTO/MEMS under Grant Nos. DABT63-98-1-0012 (Caltech) and DABT63-98-1-0010 (CWRU). The authors would like to thank Tomoyuki Yoshie for his technical assistance.

[1] M. Mehregany, C. A. Zorman, N. Rajan, and C. H. Wu, Proc. IEEE **86**, 1594 (1998).
[2] M. L. Roukes, *Technical Digest of the 2000 Solid-State Sensor and Actuator Workshop, Hilton Head Island, SC, 4–8 June 2000* (Transducer Research Foundation, Cleveland, 2000; http://arxiv.org/pdf/cond/mat/0008187.
[3] P. A. Ivanov and V. E. Chelnokov, Semicond. Sci. Technol. **7**, 863 (1992).
[4] L. Tong, M. Mehregany, and L. Matus, Appl. Phys. Lett. **60**, 2992 (1992).
[5] C. Serre, A. Perez-Rodriguez, A. Romano-Rodreguez, J. Morante, J. Esteve, and M. C. Acero, J. Micromech. Microeng. **9**, 190 (1999).
[6] A. J. Fleischman, X. Wei, C. A. Zorman, and M. Mehregany, Mater. Sci. Forum **264–268**, 885 (1998).
[7] S. Stefanescu, A. A. Yasseen, C. A. Zorman, and M. Mehregany, Technical Digest—10th International Conference on Solid State Sensors and Actuators, Sendai, Japan 7–10 June 1999, pp. 194–197.
[8] C. A. Zorman, A. J. Fleischman, A. S. Dewa, M. Mehregany, C. Jacob, and P. Pirouz, J. Appl. Phys. **78**, 5136 (1995).
[9] A. N. Cleland and M. L. Roukes, Appl. Phys. Lett. **69**, 2653 (1996); A. N. Cleland and M. L. Roukes, Sens. Actuators **72**, 256 (1999).
[10] K. E. Petersen and C. R. Giuarnieri, J. Appl. Phys. **50**, 6761 (1979).
[11] The correction factor K primarily reflects mass loading from the metallic electrode. Using values from the literature for Young's modulus of the electrode materials we deduce that the additional stiffness introduced is completely negligible.
[12] Electrodes were comprised of either Au or Al, with typical thickness ranging from 50 to 80 nm.
[13] The quantity $\sqrt{E_{\langle 100\rangle}/\rho}$ is strictly equal to neither the longitudinal sound velocity, $\sqrt{c_{11}/\rho}$, nor the transverse sound velocity, $\sqrt{c_{44}/\rho}$ for propagation along ⟨100⟩ direction of cubic crystal. Here the c's are elements of the elastic tensor and $E_{\langle 100\rangle}=(c_{11}-c_{12})(c_{11}+2c_{12})/(c_{11}+c_{12})$ for cubic crystal. See, e.g., B. A. Auld, *Acoustic Fields and Waves in Solids*, 2nd ed. (Robert E. Krieger, Malabar, FL, 1990), Vol. 1, Chaps. 6 and 7.
[14] W. R. L. Lambrect, B. Segall, M. Methfessel, and M. van Schilfgaarde, Phys. Rev. B **44**, 3685 (1991).
[15] J. J. Hall, Phys. Rev. **161**, 756 (1967).
[16] R. I. Cottam and G. A. Saunders, J. Phys. C **6**, 2105 (1973).

Downloaded 05 Jan 2001 to 131.215.106.152. Redistribution subject to AIP copyright, see http://ojps.aip.org/aplo/aplcpyrts.html.